International Information and Engineering Technology Association
Advancing the World of Information and Engineering

Traitement du Signal
Vol. 40, No. 3, June, 2023, pp. 1005-1014
Journal homepage: http://iieta.org/journals/ts

Deep Learning-Based Adaptive Beamforming for Interference Cancellation in V2I Scenarios

Prateek Bhadauria*, Ravi Kumar, Sanjay Sharma

Thapar Institute of Engineering and Technology, Patiala 147004, Punjab, India

Corresponding Author Email: pbhadauria_phd17@thapar.edu

https://doi.org/10.18280/ts.400316

Received: 2 November 2022
Accepted: 14 March 2023

Keywords:
adaptive beamforming, deep learning, LSTM, V2I, interference, 5G

ABSTRACT

The fifth-generation (5G) mobile networks rely on advanced smart antenna systems to achieve high accuracy and low latency. In vehicular-to-infrastructure (V2I) scenarios, adaptive beamforming methods play a critical role in enhancing network throughput. This paper proposes a deep learning-based adaptive beamforming technique using long short-term memory (LSTM) networks as beamformers to determine complex weights for the antenna array, thereby mitigating interference in multiuser environments. Unlike conventional minimum variance distortionless beamformers (MVDR) that require knowledge of the direction of arrival (DoA) for the desired signal, the proposed LSTM-based beamformer estimates the desired signal in the presence of interference and noise without DoA knowledge. The LSTM network is trained to predict the angles between user equipment (UE) and roadside units (RSU) using complex time series input data, resulting in a beamformed output. Simulation results demonstrate that the proposed LSTM-based beamforming approach achieves comparable performance in terms of throughput, making it a promising solution for interference cancellation in 5G V2I scenarios.

1. INTRODUCTION

The proliferation of next-generation networks has opened new avenues for V2I scenarios. Fifth-generation (5G) networks demand high data rates and low latency to meet the requirements of V2I scenarios. To address these challenges, millimeter Wave (mm-Wave) bands have been proposed to mitigate interference in vehicular communication. The compact antenna design, made possible by utilizing mm-Wave bands, enables more directional beams towards user equipment (UE). However, the propagation mechanisms of mm-Waves differ significantly from those of lower frequencies due to their shorter wavelengths. Radio waves can propagate through space in various ways, such as free-space propagation, reflection, transmission, diffraction, scattering, and wave guiding, leading to interference caused by obstacles like buildings or scattering particles [1].

Although numerous methods and techniques exist to reduce interference in 5G scenarios, adaptive beamforming (ABF) has emerged as a promising approach for V2I scenarios. This method employs compact antenna arrays (e.g., half-wavelength spacing) with efficient antenna correlation, enhancing the performance by obtaining the direction of arrival (DOA). Various beamforming techniques have been implemented for processing raw data, including acoustic signals, audio and video signals, and traditional algorithms applied in naval communication, medical imaging, and speech processing. Deep learning (DL)-based techniques have also been reported for beam management and beam selection, requiring real-time data traffic acquisition and collection, such as vehicle positions [2-5].

Recent efforts have focused on employing adaptive beamformers in various 5G use cases. Xing et al. [6] implemented a neural deep learning-based network to predict user behavior for safe and smart mobility networks. They compared the prediction performance of a basic long short-term memory (LSTM) model and a recurrent neural network (RNN) for different energy consumption levels. Ly and Yao [7] demonstrated various DL methods in 5G research by training a convolutional neural network (CNN) based on LSTM and RNN algorithms, processing data simultaneously in the form of streams. However, previous work focused on predicting trajectories for individual users rather than obtaining system network-level user distribution, which holds greater value. It was hypothesized that the DL approach could directly predict user density within the spatial domain.

As signal variations within different channel states are influenced by long and short-term dependencies, LSTM networks, a special type of deep RNN, appear to be an appropriate technique for predicting the number of user elements in each limited area due to their inherent ability to learn long-term dependencies. The LSTM network addresses the vanishing gradient problem, generating uncertainties in conventional RNN techniques and capturing long-short term spatial and temporal dependencies without affecting the optimization problem [8]. Ultimately, interference mitigation depends on the proper adjustment of antenna beamforming weights.

Various ABF techniques have been proposed for interference mitigation. Polese et al. [9] studied different machine learning (ML) algorithms for predicting the number of users at each transmitter base station and provided vehicular traffic approaches according to the key performance indicator (KPI) for users in edge controller-based 5G architectures. Liu et al. [10] investigated the detection of anomalies in Quasi-periodic time series (QTS), which are prevalent in the real world, using LSTM and CNN models. Paramasivan [11] proposed a beamforming method using hybrid neural network architecture and an intelligent direction-finding approach. To implement ABF techniques, it is crucial to update weights and steer the beam in correspondence with the dynamic environment, which helps combat interference. Thus, various co-channel interference rejection techniques have been applied to wireless systems, as reported in the study [12].

The remainder of the paper is organized as follows. Section 2 presents related work. Section 3 discusses the main contribution of the paper. The system model is described in Section 4, while the proposed methodology is formulated in Section 5. Section 6 reviews the concept of LSTM techniques, and Section 7 presents the dataset description. Results and discussion are provided in Section 8, and the paper concludes in Section 9.

2. RELATED WORKS

The beamforming patterns and waveforms design for adaptive arrays has been advent for the adaptive beamforming. In the delay and sum beamformer (DAS) which is also called Barlett beamformer, uses the delay and applies an amplitude weight to the output of each sensor results the sum of the signals in which data independent method has been used. Since the mitigation of interference is limited in this method such that the received signals are independent of data.

In current plethora, the beamforming techniques are used data dependent methods more prolifically e.g., the MVDR beamformer [13] kept the interference to signal ratio (ISR) is as high when input signal-to noise ratio (SNR) is low. Capon's method gives a consistent output to estimate the required signal in the presence of interference and noise without the knowledge of DOA. It is an adaptive technique in which steering vectors forms the patterns rely on the elements of antenna array, extracted through the full-wave analysis. In this paper the method is used to modify two well-known beamforming approaches, named the null steering beamforming and the MVDR method. Both advance techniques are applicable to model a realistic scenario of a microstrip antenna array in a planar structure, and thus, both polar angles and azimuth angles of the main lobe and nulls directions are controlled [14], In addition to it, by applying the extraction of features in hierarchical manner, the MVDR beamformer approach is capable of predicting the both temporal and spatial frameworks in the form of sequential data. By minimizing the synthetic data pre-processing tasks, the Finite impulse response (FIR) filter estimates the power spectral density of a time series signal. The FIR filter then diminishes all the input signal frequencies. The Capon beamformer has better resolution and interference mitigation quality as compared to the conventional data-independent beamformers. As the traffic data is exploded from last few years, the data dependent techniques become more notorious. The prevalent methods for the prediction of traffic are much useful in time series models, which depends on the previous values of data traffic to forecast the upcoming one [15]. Nevertheless, the recurrent neural networks (RNNs), or say simple RNN and gated recurrent unit (GRU) are the traditional methods which are not able to recognize the long-term dependencies in various scenarios of V2I. The use of these techniques shows irrelevant behaviors of moving vehicles and pedestrians on the road [16, 17]. Consequently, an explicit form of structure of RNN, the LSTM have formulated to concentrate on these limitations in context of prediction time series data [18]. Over the past few years, the LSTM network have been successfully implemented and expand its applications in traffic prediction, speech processing, robotics, natural language processing [19-21].

Moreover, evaluating RNNs in the form of LSTM, we also explain the NAR network approach as a prediction technique to diminish the interference. In a 5G based V2I network, forecasting the interference based time series signal, that are nonstationary and noisy, is a crucial problem. In this perspective both LSTM and NAR based methods are likely to give the output based on the previous values of inputs. This possibility has been explored in our present work [22, 23].

3. MAIN CONTRIBUTION

Our study introduces an innovative approach within a V2I network, which utilizes both an MVDR beamformer and a NAR-based time series forecasting method to anticipate the beamformed signal.

- The cause of pedestrian user moving with a slow speed has been considered for the first time in this paper.
- In this paper, a time delay MVDR beamforming technique is utilized to direct the beam towards the intended direction. Additionally, a Finite Impulse Response (FIR) filter is implemented at the output components of every sensor.
- The problem of mismatching of the spatial signature for non-stationary user has been resolved through the proposed approach.

4. SYSTEM MODEL

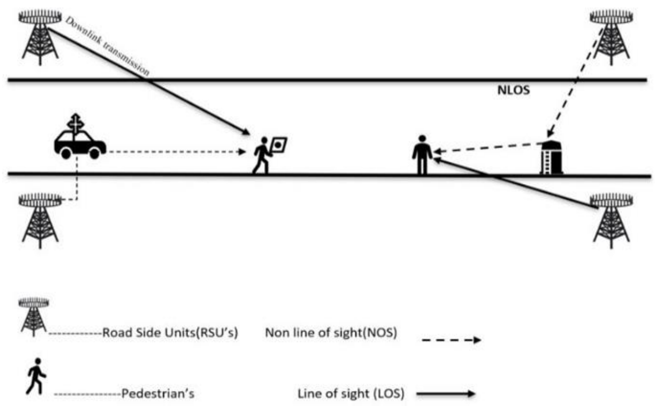

Figure 1. The proposed V2I scenario

A beamforming model for a Vehicle-to-Infrastructure (V2I) scenario using a multi-antenna configuration. Specifically, each base station (BS) consists of a uniform linear array (ULA) containing N transmitters and receivers, while the user elements (UEs) are assumed to have a single antenna and act as the beamformer for their signals is shown in Figure 1.

Thus, the signal is received at the user elements from the beamformer output is given by [24].

$$\mathrm{R(t)} = V^H \mathrm{X(t)} \tag{1}$$

where, t denotes time steps of the received signal directed at the user element based array sensor $[X(t)=X_1(t), \ldots\ldots, X_N(t)]^T$ is the Nx1 complex values of vector, $V=[v_1,\ldots v_N]^T$ which is assumed as a weight vectors of complex variables (.)H and (.)T provides the Hermitian transpose and transpose respectively.

$$\mathrm{X(t)} = \mathbf{C}_{\mathrm{d}}(\mathrm{t}) + \mathrm{I(t)n(t)} \tag{2}$$

$C_d(t)$, I(t), and n(t) are independent variables statistically for the desired user signal, interference and noise respectively. In the system model slow fading channel case is applicable, as the channel coherence time relatively large as compared to delay requirement of the V2I scenario. In this network, the phase and amplitude change imposed by the channel assumed to be constant roughly over a time period so that the vector $C_d(t)$, is given by:

$$\mathbf{C}_{\mathrm{d}}(\mathrm{t}) = \mathrm{C(t)}b_s \tag{3}$$

where, C(t) is the complex variables of the signal and b_s is its Nx1 spatial RSU's symbols which represents the wave front of UE, in such case Eq. (2) can be rewritten as:

$$\mathrm{X(t)} = \mathrm{C(t)b_s} + \mathrm{I(t)} + \mathrm{n(t)} \tag{4}$$

To obtain the beamforming vector optimally at the user, it is essential to maximize the signal to interference plus noise ratio (SINR) [25].

$$\mathrm{SINR} = \frac{\mathrm{V^H A_s V}}{\mathrm{V^H A_{i+n} V}} \tag{5}$$

where, $\mathrm{A_s} = \mathrm{E}\{\mathrm{C_d(t)C_d^H(t)}\}$.

$$\mathrm{A_{i+n}} = [\mathrm{E}\{\mathrm{I(t)} + \mathrm{n(t)}(\mathrm{I(t)} + \mathrm{n(t)}]^{\mathrm{H}} \tag{6}$$

where, A_s and A_{i+n} are NxN signal to interference plus noise covariance metrices respectively and E{.} represents expectation value used in statistics, normally A_s is considered as a rank matrix with values arbitrarily depends on the fading signal, i.e., 1≤rank $\{A_s\}$≤N. Consider a slow fading desired signal at the user side, then,

$$\mathrm{A_s} = \sigma_s^2 \mathrm{b_s b_s^H} \tag{7}$$

where, $\sigma_s^2 = \{\mathrm{E}|\mathrm{C(t)}|^2\}$, the rank $\{\mathrm{A_s}\} = 1$ is considered in this case and Eq. (5) becomes:

$$\mathrm{SINR} = \frac{\sigma_s^2 |\mathrm{V^H b_s}|^2}{\mathrm{V^H A_{i+n} V}} \tag{8}$$

By maximizing the Signal-to-Interference-plus-Noise Ratio (SINR) in Eq. (5), we can determine the optimal weight vector. This optimization approach enables us to adjust the array properties to achieve a distortionless response for the beamformed signal while simultaneously minimizing the output interference and noise power.

$$\min_{w} \; V^H \mathrm{A}_{i+n} \mathrm{V} \text{ subject to } V^H \mathrm{A}_s \mathrm{V} = 1 \tag{9}$$

Thus, when the rank of signal is 1 in this case, the Eq. (9) can be rewritten as:

$$\min_{w} \; V^H \mathrm{A}_{i+n} \mathrm{V} \text{ subject to } V^H b_s \mathrm{V} = 1 \tag{10}$$

This is called as minimum variance distortionless response (MVDR) beamforming. The explanation to Eq. (9) is given as the following eigen value problem:

$$\mathrm{A_{i+n}\, V} = \lambda\, \mathrm{A_s V} \tag{11}$$

where, λ stands eigenvalue that corresponds to Eq. (11) and are real numbers which are generally no-negative in nature that belongs to positive semidefinite of A_{i+n} and A_s, Now the optimal weight can be expressed in the form of:

$$\mathrm{V_{opt}} = \text{Ƥ}\, \{A_{i+n}^{-1} \mathrm{A}_s\} \tag{12}$$

where, Ƥ(.) is the principal eigenvector operator of matrix Eq. (12) can be simplified for rank one signal source is shown as:

$$\mathrm{V}_{opt} = P\{A_{i+n}^{-1} \mathrm{b}_s b_s^H\} = \beta\, A_{i+n}^{-1} \mathrm{b}_s \tag{13}$$

Here, the constant can be obtained from the MVDR constraint $\mathrm{v_{opt}^H b_s} = 1$, in Eq. (10) and is equal to β [26, 27].

In realistic scenarios, the correct values of matrix A_{i+n} is not obtained due to randomness of channel but it can be estimated by assumptions, so that the estimated values directed to optimization problems Eq. (9) and Eq. (10), its estimation should be used in optimization problems (9) and (10) than exact value.

Adaptive beamforming is generally applicable for canceling interference and hence it could be reasonable to base the criterion for optimization for the power at the output of the beamformer such that it is reduced by weight-set solution.

5. PROPOSED METHODOLOGY

The proposed methodology for predicting the beamformed signal can be divided into several stages, as shown in the Figure 2. Firstly, a scenario is initialized using the given data, as discussed in Section 4. Next, the data is preprocessed by normalizing the variables due to their complex nature. Following this, noise is added to the raw signal data. In the next stage, the signal is fed into a Long Short-Term Memory (LSTM) and Nonlinear Autoregressive Network (as indicated in the diagram, only LSTM is shown), and then forwarded to the fully connected layers for further processing. The weights are trained, and the network learns the dependencies of the signal based on the input parameters, including incident and azimuthal angles, as well as the number of antenna elements.

This stage is vital and little bit complex due to the configuration of network parameters, which includes the learning rate, number of hidden layers, dropout factor and amount of data is used for training and testing. The values of these parameters are interdependent, and even small changes can result in significant deviations in the output. The network reaches the output phase where it obtains the target value, and if it meets the set value, the SINR mentioned in Eq. (8) is maximized. If not, the network reverts to the LSTM model and updates its weights until it achieves the final target value. This process continues until the corresponding signals on the graph coincide with the original signal, and the desired RMSE value is calculated. To predict the required waveform of the raw signal, the LSTM network is applied.

To calculate the desired RMSE value, the predicted waveform of the input signal is generated using the LSTM network.

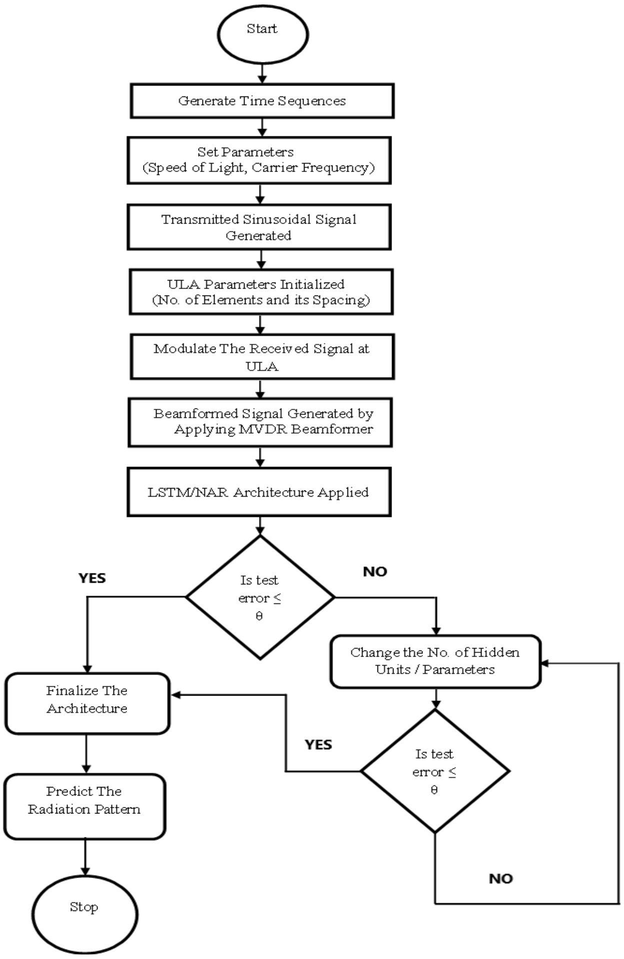

Figure 2. The proposed algorithm

The parameters used in this study follow [28, 29] and pertain to the scenario of roadside units (RSUs) with a height of approximately 25m, operating at 700MHz bandwidth, and consisting of 64 antenna elements with a noise level of 5dB. The distance between RSUs is 200m, and the user element includes 64 antenna elements operating at the same frequency with a power of 23dBm. Users may include pedestrians carrying mobile handsets with a speed of about 4km/hr and vehicles moving at a speed of 30km/hr. Because of multipath propagation, the user element has a noise figure of 7dB. In non-line-of-sight (NLOS) scenarios, the signal is distorted and causes severe interference compared to line-of-sight (LOS) scenarios. In order to reduce interference, an adaptive beamforming technique is used with an MVDR approach that places nulls at certain angles. The final beamformer relies on the regression capability of a LSTM/Neural Network-based regressor, which is necessary to meet the high SINR and throughput demands of a 5G system. This is achieved by predicting the signal in advance using MVDR weights, which automatically adjust the beam direction by modifying the azimuthal angles that are crucial to the beamforming technique. 0° angle of elevation [30]. The managerial implication is to implement the methodology according to the guidelines for evaluation of radio interface technologies for IMT-2020. The proposed scenario of Vehicular to infrastructure (V2I) supports high data rates at low latency which is according to the user's demands in multiple user environments. It enables for a wide range of services for the fifth generation (5G) mobile networks including enhanced mobile broadband services (eMBB), massive Machine Type Communications (mMTC), and URLLC (Ultra Reliable Low Latency Communications). In the V2I scenario number of roadside units (RSU's) i.e., 5G antennas are mounted and the user element (UE) vehicles are moving around it. Due to the movement of vehicles in between the RSU's and UE there is angle ambiguity occurs causing interference in the baseband signal. This interference results the low signal to interference noise ratio (SINR) and thus interference is to be detected by using the adaptive beamformer using the minimum variance distortionless response beamformer (MVDR). To predict the interference in advance a neural network- based time series forecasting method is used. It accepts the time varying data in terms of complex variables as a baseband signal and after applying the nonlinear auto regressive (NAR) neural network and long short-term memory (LSTM) based techniques, the interference is to be detected. To forecast the interference in a V2I scenario, a RMSE metric is adopted whose value should be closer to zero.

6. OVERVIEW OF LONG-SHORT TERM MEMORY (LSTM)

RNN-based LSTM networks are ideal for addressing data-dependent problems that require recognition of previous input for further processing and prediction of the next state. This allows for the structure of the hidden layer to be adjusted based on the output. The proposed LSTM structure, as depicted in Figure 3, illustrates this concept [31]. The proposed LSTM structure is a type of recurrent neural network (RNN) architecture that is designed to overcome the vanishing gradient problem in traditional RNNs. It has become popular in many natural languages processing (NLP) and speech recognition tasks due to its ability to capture long-term dependencies.

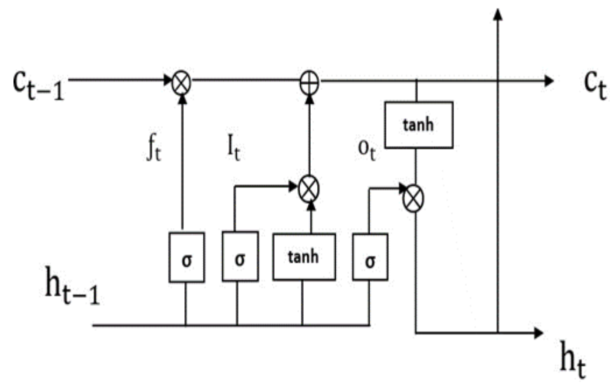

Figure 3. Basic architecture of LSTM

The basic building block of an LSTM is a memory cell, which can store information for an extended period of time. It is controlled by three gates: the input gate, output gate, and forget gate. These gates regulate the flow of information into and out of the cell, allowing the LSTM to selectively update its memory based on the input and the task at hand.

The input gate controls how much new information is allowed into the memory cell and is usually implemented as a sigmoid function. The forget gate controls how much information is removed from the cell and is also implemented as a sigmoid function. The output gate controls how much information is output from the cell and is usually implemented using a combination of a sigmoid function and a hyperbolic tangent (tanh) function. The structure of an LSTM typically consists of multiple memory cells arranged in a chain, with each cell connected to the previous and next cells via the gates.

The input to the LSTM is usually a sequence of vectors, and the output is a sequence of vectors that represent the hidden state of the LSTM at each time step. Overall, the LSTM architecture allows for more precise control over the flow of information in and out of the memory cells and has been shown to be highly effective for a wide range of sequence prediction tasks.

The gate I_t acts an input gate decides which part of input is get processed further to update the cell. After updating the cell the forget gate f_t take decision which part of the earlier cell will be dumped out while the output gate O_t can be considered as output. Where x_t and C_t denote the input data at time t and the memory unit respectively. Assume that x_t and h_t denotes the inputs and outputs at present time-instance, h_{t-1} corresponds to output of the previous instance of time, denotes the activation function known as sigmoid activation function, and Ⓢ denotes the Hadamard product, the basic representations of the LSTM model are shown in Figure 3.

$$f_t = \sigma\left(W_f\, x_t + U_f h_{t-1} + b_f\right) \tag{14}$$

$$I_t = \sigma(W_I x_t + U_I h_{t-1} + b_I) \tag{15}$$

$$O_t = \sigma(W_o x_t + U_o h_{t-1} + b_o) \tag{16}$$

$$\tilde{C}=f_t Ⓢ C_{t-1} \tag{17}$$

$$h_t=O_t Ⓢ \tanh C_t \tag{18}$$

(W_f, W_I, W_o), (U_f, U_I, U_o) and (b_f, b_I, b_o) stands for the recurrent weights, input weights, and biases for each gate respectively. As precisely, the LSTM networks consists of different replicas of standard memory blocks, and every component of block comprised a memory cell and three different types of gates (input gate, output gate, and forget gate. The cell is the essential portion of LSTM memory and is viable for transfer of data into different steps of time [32].

This network resolves the vanishing gradient problem and provides wide range of tuning parameters like learning rate, input, output and biases. They also handled the long-term dependencies in a very effective manner. It can handle complex, non-linear, sequential data in a very simpler form. But they are not suitable for online learning task like prediction and classification in which sequential data is not available. It needs high memory bandwidth because linear layers are available in cells state, so the implementation hardware system is inefficient.

7. DATASET DESCRIPTION

The dataset consists of Nx1 time series-based vector input represents weights of beamformer corresponds to N rows contains one column and 361 values was considered as a beamformed signal output. The departed signal from the transmitter having complex value is received on an array of 64 elements from the direction of azimuthal angle 0° and 45° elevation. To calculate the mean square error, the weights of the signal impinging on an array with the addition of noise is generated as a data which is based on the scenario discussed in section 3. Each point of data are complex values denoted by either a two-dimensional coordinate according to the requirement of spatial geometry for V2I applications. The partitioning of the data to train a LSTM network for the prediction of interference is divided into three parts: (I) A layer acts as an input is connected completely which is a sequences of positions of the moving pedestrian and vehicles, such that each value corresponds to a multi-dimensional vector; (II) The processed sequence then sent to the critical section of the interference model; (III) finally, the fully connected output layer maps the last LSTM output layer at each time-step. It is necessary to train the data for reducing the loss function in terms of normalize mean square error (NMSE) where the input Nx1 one dimensional series vector contains the complex value weights w_i. The training signal is considered as the received signal impinging on the array to train the network. Now apply the time series forecasting LSTM based method to predict the future values of time steps using the sequence to sequence regression concept. Therefore, the LSTM network learn and predict the values of the desired signal in succeeding time step of the input sequence. After that LSTM predicted the beamformed signals corresponds to the output as a number of beamforming weights. The output of the network is in the form of cell array in which every element is a single time step. Reshaping of the data is a row vector and then data splitting is done in to training and testing phase in 80-20% ratio, after that to avoid the overfitting data is fit into the network. The standard form of training data is set to have zero mean and unity variance. During the testing phase the data should be in the same format as the parameters of training data are set for the prediction. Train Network function is used in MATLAB 2020a to train the data. Here the outcome of the training is used for beamformed signal to predict the three cells, since they have been deployed in to three different regions, the scattered interference profiles in terms of amplitude and number of iterations of signal at the RSU's. The forecast is one-step ahead for the prediction of number of iterations with the oscillating nature of the interference, implies that we are using previous values to estimate the DoA for the next time slot. Here, the predictions are showing good results than past calculations when updates the network with observed values of parameters than the predicted values. So, to compute the performance of the proposed architecture, we compute the interference on average basis, thus the data is synthetically generated data and not easy to calculate at instances, so we choose the root mean square error (RMSE) of this quantity. For the ease of calculation, it is then again normalized which is the metric to measure accuracy of the prediction algorithm, and is given by:

$$\mathrm{RMSE}=\sqrt{\frac{1}{\bar{\mathrm{x}}}\frac{\sum_{\mathrm{t}=1}^{\mathrm{M}}\ (\tilde{\mathrm{x}}_{\mathrm{t}}-\mathrm{x}_{\mathrm{t}})^2}{\mathrm{M}}} \tag{19}$$

Here, M is number of instances of total values, $\tilde{\mathrm{x}}_{\mathrm{t}}$ and x_{t} is the predicted value at time t and $\bar{\mathrm{x}}$ denotes its mean. By using this method, it is easier for comparison of results showing the accuracy of the proposed technique with the existing one. The implementation of the interference prediction algorithm is done in MATLAB 2020a version.

8. RESULTS AND DISCUSSION

We discuss the performance of two networks in terms of normalized power and RMSE in the forecast phase. Figures shows the comparative study of root mean square error values for NAR model with the LSTM model. The impact of significant array parameters on the predictor's error performance has been illustrated. This section gives valuable insights on the optimal array parameters that lead to a nearly perfect beamformed signal, thus enhancing network performance. It accomplishes this by appropriately training weights to predict the interference signal and displaying the network's error output. Figure 4a shows the baseband signal which is applied at the input of the MVDR beamformer. A comparative inspection of Figure 4b and Figure 4c. When the incident angle parameter of the received signal was changed, it was observed that the beamformed signal predicted by NAR showed greater similarity to the baseband signal than the one predicted by LSTM.

It is evident from a sharper dip in the normalized power of the beamformed signal in Figure 4c, the reason for a less similar forecasted beam pattern in the case of LSTM can be attributed to its more intricate training and updating process, which is inherent to the LSTM module. The correlation between the forecasted signal and the baseband signal's similarity was found to be directly linked to the RMSE obtained during the testing phase. As a result, only the RMSE values have been presented for the sake of conciseness. Figure 4c shows a portion that was predicted by the NAR regressor with a sufficiently low error in the testing phase. We can observe from Figure 4d and Figure 4e the effect of weight update on the prediction performance of LSTM network. The top section displays the normalized power of the predicted signal before and after the update, while the bottom section demonstrates the impact of the update on the RMSE during the testing phase, which is significantly reduced by several orders of magnitude in the latter case. The forecasted results shown in Figure 4a to Figure 4e corresponds to the case when received signal incident angle was varied from 40 to 100 degrees keeping all other parameters fixed. In Figure 4d training signal before forecast gives the nulls or the dip of signal in the range between 55 to 60. By visualizing the graph also depicts the slight variation between the observed signal and forecasted signal. So, the resultant RMSE value is 5.176 which is not feasible for the network performance. While updating the weights of LSTM network of the Figure 4e the observed and predicted values of the signal coincides with each other, thus it gives better performance as earlier when it was not updating the weights. After updating the weights, the RMSE value reached closer to zero, which is 1.2475. The vital role of an LSTM model is governed by a memory cell called a 'cell state'. A cell state determines the requirement from previous cell state to next cell state. It always updating the data capable to manage which information is useful in the system and which information is dropped out. If some information is required it will update or add the information with the help of three gates. So, we have three gates forget gate, input gate and output gate. All three gates are placed inside the LSTM cell.

The RMSEs of LSTM and NAR regressor are depicted in Figure 5a when incident angle was varied from 40 to 100 degrees, it is considered as a primary input showing the three basic metric in terms of min, average and maximum value. So, it can be observed that the RMSEs of both regressor are comparable from Figure 5a and 5b. Since, the experiments were done several times with k-fold cross validation method (k=10), in Figure 5a, average value of the RMSE obtained in k-folds has been plotted. For the reader's reference, Figure 5b showing maximum, minimum, and average values of the RMSE obtained using NAR network. Similarly, the RMSEs obtained when primary input for the beamformer was azimuthal angle have been shown in Figure 6a to 6c. In this case NAR exhibits better performance than LSTM. Also, Table 1 depicts the corresponding azimuthal angle span.

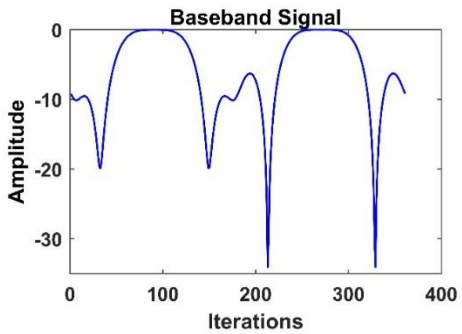

Figure 4a. Baseband signal

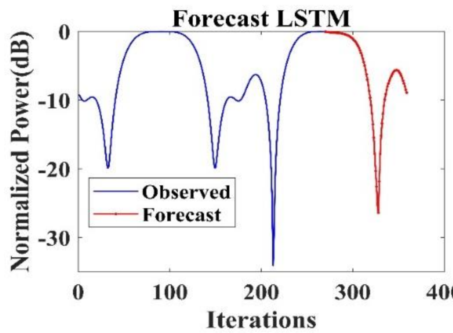

Figure 4b. LSTM forecasted beamformed signal

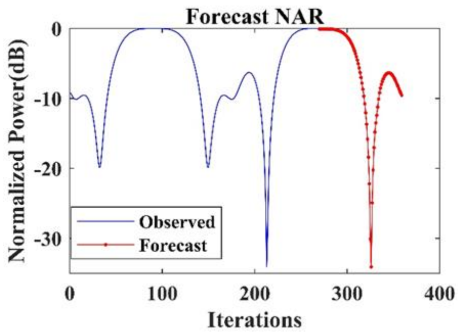

Figure 4c. Forecasted NAR signal

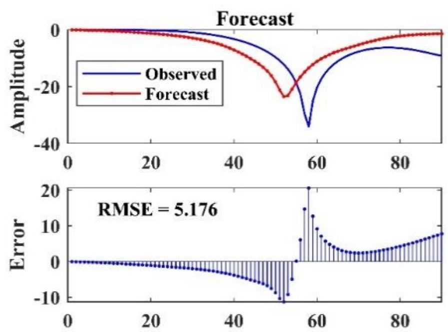

Figure 4d. Training signal before forecast

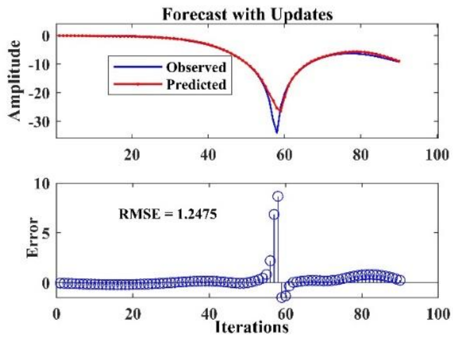

Figure 4e. Forecasted signal after training

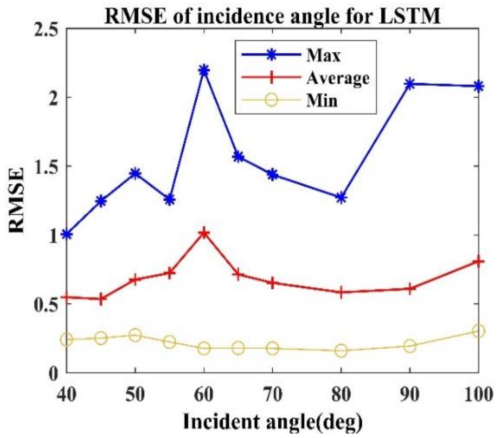

Figure 5a. RMSE's of incidence angle (LSTM)

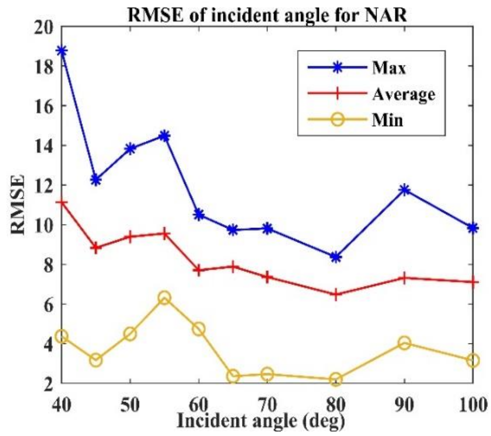

Figure 5b. RMSE's of incidence angle (NAR)

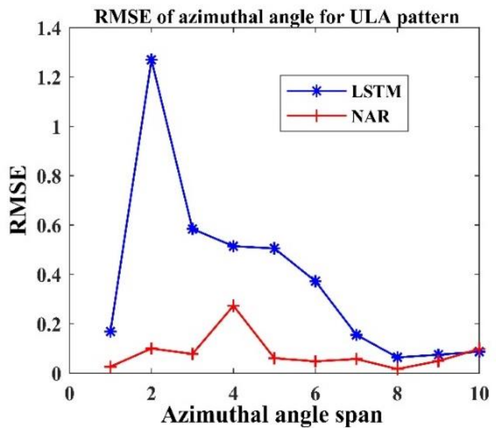

Figure 6a. RMSE comparison (LSTM and NAR)

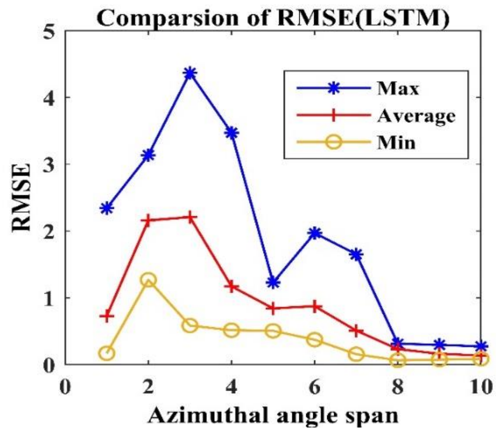

Figure 6b. RMSE of azimuthal angle (LSTM)

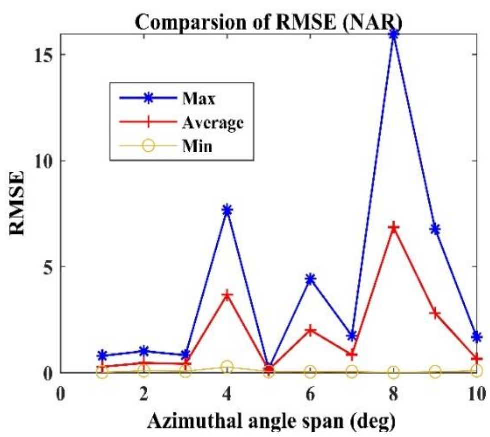

Figure 6c. RMSE of azimuthal angle (NAR)

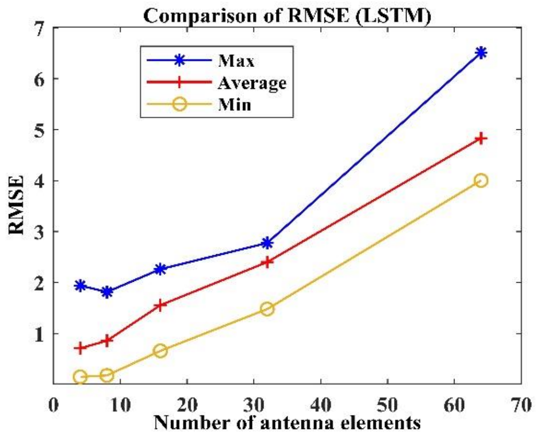

Figure 7a. RMSE for no. of elements (LSTM)

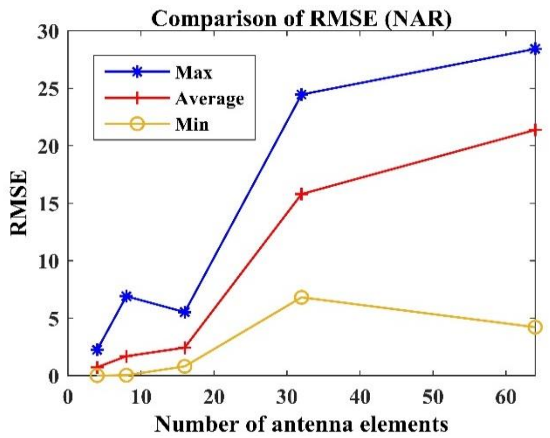

Figure 7b. RMSE for no. of elements (NAR)

Table 1. Designation for azimuthal angles

Angle Span	Designated as
-30 to+30	1
-45 to+45	2
-60 to+60	3
-70 to+70	4
-80 to+80	5
-90 to+90	6
-100 to+100	7
-110 to+110	8
-120 to+120	9
-130 to+130	10

The NAR is a is a non-parametric method that can support dynamic inputs based on times series data. It can also perform multistep predictions for closed loop networks. This network can continue to predict the output values by using internal feedback even when external feedback is missing. But it cannot work on stationary data, otherwise there is no meaning for the approximation of neural networks. The model uses the number of delays which causes the system more complex, so it affects the efficiency of learning. It is not applicable for open loop networks.

It lags The NAR predicts the future values of a time series data on the basis of past values. It. It can fulfill the universal approximation theorem for neural network. Perhaps the important significant advantage of LSTM scheme can be observed from Figure 7a and Figure 7b where number of elements of antenna are varied from 4 to 64. Here, Root means square error of NAR regressor is larger than the LSTM regressor, thus from the respective figures depicting that the LSTM performs better as compared to NAR. It is probable that the LSTM module handles the complexity arising from increase in the number of antenna elements, while the NAR module falls short since it lacks the ability to learn dependencies. Therefore, in a practical scenario, where, the antenna array/sensor elements are huge in numbers, it would be advisable to apply an LSTM based forecast stage for beamforming.

9. CONCLUSIONS

Based on the findings presented in the preceding section, it can be inferred that neural network-based regressors can effectively predict beamformed signals. Data produced by conventional beamforming techniques, such as MVDR, can be utilized for training purposes. Additionally, LSTM shows potential in predicting beamformed signals since there are various short- and long-term dependencies present in V2I scenarios that the regressor must learn. In this study, LSTM performed better than NAR-based regressors, particularly when the number of antenna elements was high, for the considered V2I scenario. In the future, there is an opportunity to optimize the architecture of the LSTM module with the goal of reducing computational complexity while improving the accuracy of the beamforming forecasts. In this paper real time data collection is a tedious task, due to the installation of cloud servers and confined to limited resources. if the vehicular communication scenario will make it more complex the cost of sharing the messages between RSU's and UE is not easily feasible, so it is assumed that the information is not delay and error free. For high mobility vehicular communication scenario, it is important to think about the practical limitation imposed by the harsh V2I environment. Furthermore, exploring the wideband beamforming techniques with deep reinforcement learning agent-based system network appears to be an interesting future research plethora.

REFERENCES

[1] Chetlur, V.V., Dhillon, H.S. (2019). Coverage and rate analysis of downlink cellular vehicle-to-everything (C-V2X) communication. IEEE Transactions on Wireless Communications, 19(3): 1738-1753. https://doi.org/10.1109/TWC.2019.2957222

[2] Shi, S.G., Gao, Y., Yang, D.S., Shi, J., Tian, D.Y. (2021). An improved generalized inverse beamforming-noise source localization method using acoustic vector sensor arrays. IEEE Sensors Journal, 21(14): 16222-16235. https://doi.org/10.1109/JSEN.2021.3076187

[3] Rosado-Sanz, J., Jarabo-Amores, M.P., De la Mata-Moya, D., Rey-Maestre, N. (2022). Adaptive beamforming approaches to improve passive radar performance in sea and wind farms' clutter. Sensors, 22(18): 6865. https://doi.org/10.3390/s22186865

[4] Ma, Y.G., Zeng, Y.H., Sun, S.M. (2022). A deep learning based super resolution DOA estimator with single snapshot mimo radar data. IEEE Transactions on Vehicular Technology, 71(4): 4142-4155. https://doi.org/10.1109/TVT.2022.3151674

[5] Wang, Y. (2020). Moving vehicle detection and tracking

based on video sequences. Traitement du Signal, 37(2): 325-331. https://doi.org/10.18280/ts.370219

[6] Xing, Y., Lv, C., Mo, X.Y., Hu, Z.X., Huang, C., Hang, P. (2021). Toward safe and smart mobility: Energy-aware deep learning for driving behavior analysis and prediction of connected vehicles. IEEE Transactions on Intelligent Transportation Systems, 22(7): 4267-4280. https://doi.org/10.1109/TITS.2021.3052786

[7] Ly, A., Yao, Y.D. (2021). A review of deep learning in 5G research: Channel coding, massive MIMO, multiple access, resource allocation, and network security. IEEE Open Journal of the Communications Society, 2: 396-408. https://doi.org/10.1109/OJCOMS.2021.3058353

[8] Echigo, H., Cao, Y.W., Bouazizi, M., Ohtsuki, T. (2021). A deep learning-based low overhead beam selection in mmWave communications. IEEE Transactions on Vehicular Technology, 70(1): 682-691. https://doi.org/10.1109/TVT.2021.3049380

[9] Polese, M., Jana, R., Kounev, V., Zhang, K., Deb, S., Zorzi, M. (2020). Machine learning at the edge: A data-driven architecture with applications to 5G cellular networks. IEEE Transactions on Mobile Computing, 20(12): 3367-3382. https://doi.org/10.1109/TMC.2020.2999852

[10] Liu, F., Zhou, X.S., Cao, J.L., Wang, Z., Wang, T.B., Wang, H., Zhang, Y.C. (2020). Anomaly detection in quasi-periodic time series based on automatic data segmentation and attentional LSTM-CNN. IEEE Transactions on Knowledge and Data Engineering, 34(6): 2626-2640. https://doi.org/10.1109/TKDE.2020.3014806

[11] Paramasivan, S.K. (2021). Deep learning based recurrent neural networks to enhance the performance of wind energy forecasting: A review. International Information and Engineering Technology Association, Revue d'Intelligence Artificielle, 35(1): 1-10. https://doi.org/10.18280/ria.350101

[12] Biswas, S., Singh, U., Nag, K. (2021). Multi-layer perceptron-based beamformer design for next-generation full-duplex cellular systems. In 2021 IEEE/ACIS 22nd International Conference on Software Engineering, Artificial Intelligence, Networking and Parallel/Distributed Computing (SNPD), IEEE, 49-55. https://doi.org/10.1109/SNPD51163.2021.9704974

[13] Ramezanpour, P., Mosavi, M.R. (2020). Two-stage beamforming for rejecting interferences using deep neural networks. IEEE Systems Journal, 15(3): 4439-4447. https://doi.org/10.1109/JSYST.2020.3034957

[14] Zaharis, Z.D., Gravas, I.P., Lazaridis, P.I., Yioultsis, T.V., Xenos, T.D. (2022). Improved beamforming in 3D space applied to realistic planar antenna arrays by using the embedded element patterns. IEEE Transactions on Vehicular Technology, 71(6): 6145-6157. https://doi.org/10.1109/TVT.2022.3155966

[15] Zhao, Z., Chen, W.H., Wu, X.M., Chen, P.C.Y., Liu, J.M. (2017). LSTM network: A deep learning approach for short-term traffic forecast. IET Intelligent Transport Systems, 11(2): 68-75. https://doi.org/10.1049/iet-its.2016.0208

[16] Ma, X.L., Tao, Z.M., Wang, Y.H., Yu, H.Y., Wang, Y.P. (2015). Long short-term memory neural network for traffic speed prediction using remote microwave sensor data. Transportation Research Part C: Emerging Technologies, 54: 187-197. https://doi.org/10.1016/j.trc.2015.03.014

[17] Zhang, L., Zhang, H.T., Jiang, Y., Wu, Z.Q. (2020). Intelligent and reliable deep learning LSTM neural networks-based OFDM-DCSK demodulation design. IEEE Transactions on Vehicular Technology, 69(12): 16163-16167. https://doi.org/10.1109/TVT.2020.3022043

[18] Mallioras, I., Zaharis, Z.D., Lazaridis, P.I., Pantelopoulos, S. (2022). A novel realistic approach of adaptive beamforming based on deep neural networks. IEEE Transactions on Antennas and Propagation, 70(10): 8833-8848. https://doi.org/10.1109/TAP.2022.3168708

[19] Bogale, T.E., Wang, X.B., Le, L.B. (2020). Adaptive channel prediction, beamforming and scheduling design for 5G V2I network: Analytical and machine learning approaches. IEEE Transactions on Vehicular Technology, 69(5): 5055-5067. https://doi.org/10.1109/TVT.2020.2975818

[20] Baldi, S., Michailidis, I., Ntampasi, V., Kosmatopoulos, E.B., Papamichail, I., Papageorgiou, M. (2015). Simulation-based synthesis for approximately optimal urban traffic light management. In 2015 American Control Conference (ACC), IEEE, pp. 868-873. https://doi.org/10.1109/ACC.2015.7170843

[21] Sohrabi, F., Chen, Z.L., Yu, W. (2021). Deep active learning approach to adaptive beamforming for mmWave initial alignment. IEEE Journal on Selected Areas in Communications, 39(8): 2347-2360. https://doi.org/10.1109/JSAC.2021.3087234

[22] Qazani, M.R.C., Asadi, H., Lim, C.P., Mohamed, S., Nahavandi, S. (2021). Prediction of motion simulator signals using time-series neural networks. IEEE Transactions on Aerospace and Electronic Systems, 57(5): 3383-3392. https://doi.org/10.1109/TAES.2021.3082662

[23] Misra, A., Sarma, M.P., Sarma, K.K., Mastorakis, N. (2022). Temporal deep learning assisted UAV communication channel model for application in EH-MIMO-NOMA set-up. Journal of Communications and Networks, 24(2): 166-183. https://doi.org/10.23919/JCN.2021.000045

[24] Huang, H.J., Yang, J., Huang, H., Song, Y.W., Gui, G. (2018). Deep learning for super-resolution channel estimation and DOA estimation based massive MIMO system. IEEE Transactions on Vehicular Technology, 67(9): 8549-8560. https://doi.org/10.1109/TVT.2018.2851783

[25] Zhang, L., Huang, L., Li, B., Huang, M., Yin, J.W., Bao, W.M. (2019). Fast-moving jamming suppression for UAV navigation: A minimum dispersion distortionless response beamforming approach. IEEE Transactions on Vehicular Technology, 68(8): 7815-7827. https://doi.org/10.1109/TVT.2019.2924951

[26] Venkategowda, N.K.D., Tandon, N., Jagannatham, A.K. (2014). MVDR-based multicell cooperative beamforming techniques for unicast/multicast MIMO networks with perfect/imperfect CSI. IEEE Transactions on Vehicular Technology, 64(11): 5160-5176. https://doi.org/10.1109/TVT.2014.2377297

[27] Huang, Y.W., Zhou, M.K., Vorobyov, S.A. (2019). New designs on MVDR robust adaptive beamforming based on optimal steering vector estimation. IEEE Transactions on Signal Processing, 67(14): 3624-3638. https://doi.org/10.1109/TSP.2019.2918997

[28] Series, M. (2017). Guidelines for evaluation of radio interface technologies for IMT-2020. Report ITU-R, M.2412-0.

[29] Garcia, M.H.C., Molina-Galan, A., Boban, M., Gozalvez, J., Coll-Perales, B., Şahin, T., Kousaridas, A. (2021). A tutorial on 5G NR V2X communications. In IEEE Communications Surveys & Tutorials, 23(3): 1972-2026. https://doi.org/10.1109/COMST.2021.3057017

[30] Zhang, Y., Chen, J., You, T., Zhang, Y., Liu, Z., Du, C. (2023). Energy-aware optimization of connected and automated electric vehicles considering vehicle-traffic nexus. IEEE Transactions on Industrial Electronics, pp. 1-10. https://doi.org/10.1109/TIE.2023.3245204

[31] Smagulova, K., James, A.P. (2019). A survey on LSTM memristive neural network architectures and applications. The European Physical Journal Special Topics, 228(10): 2313-2324. https://doi.org/10.1140/epjst/e2019-900046-x

[32] Liu, Y.N., Wang, X.B., Boudreau, G., Sediq, A.B., Abou-zeid, H. (2020). Deep learning based hotspot prediction and beam management for adaptive virtual small cell in 5G networks. IEEE Transactions on Emerging Topics in Computational Intelligence, 4(1): 83-94. https://doi.org/10.1109/TETCI.2019.2926769